J Bioenerg Biomembr (2007) 39:291–300
DOI 10.1007/s10863-007-9091-0

ORIGINAL PAPER

IF_1 distribution in HepG2 cells in relation to ecto–F_0F_1ATPsynthase and calmodulin

Stefania Contessi · Marina Comelli · Sara Cmet · Giovanna Lippe · Irene Mavelli

Received: 8 January 2007 / Accepted: 9 May 2007 / Published online: 13 September 2007

Abstract F_0F_1ATPsynthase is now known to be expressed as a plasma membrane receptor for several extracellular ligands. On hepatocytes, ecto–F_0F_1ATPsynthase binds apoA–I and triggers HDL endocytosis concomitant with ATP hydrolysis. Considering that inhibitor protein IF_1 was shown to regulate the hydrolytic activity of ecto–F_0F_1ATPsynthase and to interact with calmodulin (CaM) in vitro, we investigated the subcellular distributions of IF_1, calmodulin (CaM), OSCP and β subunits of F_0F_1ATPsynthase in HepG2 cells. Using immunofluorescence and Western blotting, we found that around 50% of total cellular IF_1 is localized outside mitochondria, a relevant amount of which is associated to the plasma membrane where we also found Ca^{2+}–CaM, OSCP and β. Confocal microscopy showed that IF_1 colocalized with Ca^{2+}–CaM on plasma membrane but not in mitochondria, suggesting that Ca^{2+}–CaM may modulate the cell surface availability of IF_1 and thus its ability to inhibit ATP hydrolysis by ecto–F_0F_1ATPsynthase. These observations support a hypothesis that the IF_1–Ca^{2+}–CaM complex, forming on plasma membrane, functions in the cellular regulation of HDL endocytosis by hepatocytes.

Keywords HepG2 cells · Natural inhibitor protein IF_1 · Calmodulin (CaM) · Ecto–F_0F_1ATPsynthase · Mitochondrion · Plasma membrane

S. Contessi · M. Comelli · S. Cmet · G. Lippe · I. Mavelli (✉)
Department of Biomedical Sciences and Technologies,
MATI Centre of Excellence, University of Udine,
Piazzale Kolbe 4,
33100 Udine, Italy
e-mail: imavelli@mail.dstb.uniud.it

Abbreviations

CaM	calmodulin
IF_1	F_0F_1ATPsynthase inhibitor protein
F_1	soluble isolated F_1 domain

Introduction

Traditionally, F_0F_1ATPsynthase expression has been considered to be confined to mitochondria, where the F_1 catalytic domain (subunit composition $\alpha_3\beta_3\gamma\delta\varepsilon$) aerobically synthesizes cellular ATP using energy from the transmembrane proton motive force generated by F_0 domain (bovine subunits a, b, c, OSCP, d, e, f, g, F_6 and A6L; Boyer 1997). Recently, components of F_0F_1ATPsynthase (ecto–F_0F_1ATPsynthase) have been identified as cell-surface receptors for ligands apparently unrelated to ATP synthesis (reviewed in Champagne et al. 2006). In particular, ecto–F_0F_1ATPsynthase of endothelial cells binds angiostatin and modulates endothelial cell proliferation and differentiation (Moser et al. 1999, 2001; Burwick et al. 2005). In tumors, ecto–F_0F_1ATPsynthase and apolipoprotein A–I (apoA–I) are bound by the antigen receptor of circulating cytotoxic lymphocytes of the γδ subtype and thus promote innate tumor cell recognition and lysis (Scotet et al. 2005). On hepatocytes, the complex is a high-affinity apoA–I receptor that triggers endocytosis of holo–HDL particles by a mechanism depending on ADP generation (Martinez et al. 2003) and involving the G-protein coupled P2Y13 receptor (Jacquet et al. 2005).

Research into HDL endocytosis by hepatocytes demonstrated not only the important role of the ATP hydrolytic activity of ecto–F_0F_1ATPsynthase but also the regulation of

this enzyme activity by its natural inhibitory protein IF_1. In particular, addition of exogenous IF_1 reduced the hydrolytic activity of plasma membrane ATPsynthase and decreased HDL_2 endocytosis by about 50% in perfused rat liver (Martinez et al. 2003). More recently, endogenous IF_1 has been identified on the surface of endothelial cells (Burwick et al. 2005) where it accumulated after TNF-α stimulation (Cortes-Hernandez et al. 2005), supporting a physiological role for ecto–IF_1. The cell-surface function of IF_1 mimics its inhibition of ATPase activity of mitochondrial F_0F_1ATP-synthase under conditions of energy deficiency (Green and Grover 2000) that occur both in vitro and in vivo during ischemia and ischemic preconditioning in mammalian heart (Di Pancrazio et al. 2004; Penna et al. 2004) and under preconditioning conditions consequent to pharmacologic treatment (Contessi et al. 2005; Comelli et al. 2007).

IF_1 is a basic α-helical protein that displays a high degree of sequence similarity in a wide range of species. IF_1 binds in the α_{DP}–β_{DP} interface of F_1 catalytic sector (Cabezon et al. 2003) in a 1:1 ratio (Green and Grover 2000). As previously reported by the Pedersen and Carafoli groups (Pedersen and Hullihen 1984; Schwerzmann et al. 1985) and further characterized by us (Contessi et al. 2005), IF_1 is a target of calmodulin (CaM), a ubiquitous and highly conserved protein in all eukaryotes that functions as a calcium sensor (Chin and Means 2000). CaM is a heat-stable protein with four conserved helix–loop–helix structures (EF-hand motifs) that each bind a single calcium ion. CaM interacts with a large number of structurally and functionally unrelated proteins, including metabolic enzymes, structural proteins, transcription factors, ion channels and pumps, and modulates a wide range of cellular processes in response to calcium (Yamniuk and Vogel 2004). Our previous in vitro research concerning IF_1 binding to CaM clarified that the interaction is Ca^{2+}-dependent and occurs with a 1:1 ratio over a wide pH range (Contessi et al. 2005). We also identified a target sequence on IF_1 for CaM binding, and proposed that the IF_1–Ca^{2+}–CaM complex forms outside mitochondria (Contessi et al. 2005). Although IF_1 is encoded by a nuclear gene (Walker et al. 1987), little is known about IF_1 cytosolic trafficking and the mechanisms and proteins involved in this process.

In light of this knowledge, we studied the subcellular distribution of IF_1 in human hepatocarcinoma HepG2 cells, already shown to express F_0F_1ATPsynthase subunits α, β, δ, γ, b, d, e, F6 and OSCP on the plasma membrane (Bae et al. 2004). We aimed to determine if, also in HepG2 cells, IF_1 is associated with the plasma membrane and, if so, whether it colocalizes with subunits of ecto–F_0F_1ATPsynthase or with CaM. These experiments were performed to shed light on the possible role of the IF_1–Ca^{2+}–CaM complex in the regulation of HDL endocytosis by hepatocytes.

Materials and methods

Materials

Primary antibodies used in this study were: mouse anti-IF_1 and mouse anti-OSCP (Molecular Probes, Eugene, Oregon, USA); mouse anti-Ca^{2+}–CaM (USBiological, P.O. Box 261 Swampscott, MA, USA); mouse anti-CaM and mouse anti-α_1 subunit of Na^+K^+ATPase (AbCam, Cambridge, UK); rabbit anti-apoptosis inducing factor (anti-AIF; Chemicon International, Temecula, CA, USA); rabbit anti-IF_1 (kindly provided by D. Harris, Department of Biochemistry, University of Oxford, UK); rabbit anti-β subunit of F_0F_1ATPsynthase (kindly provided by Dr. F. Dabbeni-Sala, Department of Pharmacology, University of Padua, Italy); and rabbit anti-RAIDD (kindly provided by C. Brancolini, Department of Biomedical Sciences and Technologies, University of Udine, Italy). Horseradish peroxidase (HRP)-conjugated goat anti-mouse and anti-rabbit IgG, fluorescein isothiocyanate (FITC)-conjugated goat anti-mouse IgG and goat anti-rabbit IgG, and alexa fluor-conjugated goat anti-rabbit IgG were purchased from Chemicon. Mitotracker Red CMXRos was from Molecular Probes. Molecular weight standards and blotting-grade non-fat dry milk were from Bio-Rad (Hercules, CA, USA). SuperSignal West Dura chemiluminescent substrate was obtained from Pierce (Rockford, IL, USA). Trypan blue was purchased from Biochrom (Berlin, Germany). Cell culture medium was obtained from Euro-Clone (Devon, UK). All other reagents were purchased from Sigma (St. Louis, MO, USA).

Cell culture

Human hepatocarcinoma HepG2 cells at low passage number (4–10 passages) were maintained in Dulbecco's modified Eagle's medium (DMEM), supplemented with 10% fetal bovine serum (FBS), 4 mM glutamine, 100 μU/ml penicillin, 100 μg/ml streptomycin and 10 μg/ml gentamycin. Cells were grown at 37 °C in a humidified atmosphere with 5% CO_2. Prior to using cells for immunofluorescence or fractionation protocols, we ascertained that viability was >95% as determined by the trypan blue dye exclusion test.

Flow cytofluorimetry

Confluent HepG2 cells were washed twice in phosphate–buffered saline pH 7.4 (PBS), detached with trypsin-EDTA, fixed in 4% paraformaldehyde in PBS for 15 min, and washed twice in blocking solution (PBS containing 1% BSA) as described by Martinez and co-workers (Martinez et al. 2003). Fixed cells were incubated in blocking solution

plus primary antibodies against F_0F_1ATPsynthase subunits OSCP and β, IF_1 and Ca^{2+}–CaM (1:200) at 20 °C for 1 h. The cells were then washed in blocking solution and incubated with FITC-conjugated goat anti-mouse IgG or anti-rabbit IgG (1:1,000) at 20 °C for 30 min. After washing in blocking solution, cells were suspended to 2×10^6 cell/ml in PBS and were analyzed with a FACScan flow cytometer (Becton–Dickinson, New York, USA) equipped with a single 488 nm argon laser.

Cells incubated with antibodies to α_1 subunit of Na^+K^+ATPase, a plasma membrane marker (Zhao and Hundal 2000), and to AIF, resident in the mitochondrial intermembrane space (Joza et al. 2001), were used as positive controls. Cells treated with only secondary antibody served as negative controls.

Confocal microscopy

HepG2 ($1–2\times10^4$ cells) were plated in complete medium on 20-mm glass bottom dishes or on glass coverslips, grown overnight and treated as in Martinez et al. (2003). When indicated, cells were incubated with 100 nM Mitotracker Red for 15 min under growth conditions. Cells were washed in PBS, fixed with 4% paraformaldehyde in PBS for 20 min at 37 °C and washed three times with PBS. After fixation, Mitotracker Red-labelled cells were permeabilized with 0.2% Triton X-100 in PBS for 5 min and washed three times with PBS. Cells were incubated overnight with antibodies against F_0F_1 subunits OSCP and β, IF_1 and CaM (1:200) in blocking solution at room temperature; cells incubated with anti-α_1 subunit of Na^+K^+ATPase (1:200) and anti-AIF (1:200) served as controls. For some colocalization experiments, cells were incubated simultaneously with one monoclonal and one polyclonal antibody. After three washes with blocking solution, cells were stained with appropriate secondary antibodies: FITC-conjugated goat anti-mouse or anti-rabbit IgG, or alexa fluor-conjugated anti-rabbit IgG (1:1,000), for 3 h at room temperature. After washing, cells were examined under a laser scanning microscope (Leica TCS NT) equipped with a 488–534 nm Ar and a 633 nm He–Ne laser.

Subcellular fractionation

Sub-confluent HepG2 cells were washed twice in PBS, detached with trypsin–EDTA, pelleted at 280 g for 5 min at 20 °C, and resuspended to $1–2\times10^7$ cells/ml in sonication buffer (250 mM sucrose, 1% BSA, 2 mM EDTA, pH 7.4) with protease inhibitors (4-[2 aminoethyl]-benzenesulfonyl fluoride (AEBSF), pepstatin A, E-64, bestatin, leupeptin and aprotinin).

Sonication was chosen as a method for cell breakage because it permits obtaining both intact mitochondria (Abou-Khalil et al. 1985) and uncontaminated plasma membranes (Tietz et al. 2005). Cell suspensions were sonicated on ice with three 5-s bursts at 30-s intervals, resulting in 95% disrupted cells. Cell fractionation aimed to maximize purity rather than protein recovery. All procedures were performed at 4 °C or on ice. Sonicated cells were centrifuged at 280 g for 10 min to pellet unbroken cells and large membrane sheets (step 1). According to Bae et al. (2004), the supernatant was centrifuged at 1,500 g for 10 min to separate the nuclear fraction plus residual membrane sheets from the post-nuclear fraction (step 2). The pellet was suspended in 250 mM STM buffer (0.25 M sucrose, 5 mM Tris–HCl pH 7.4, 1 mM $MgCl_2$), 2 M STM buffer was added to obtain a final concentration of 1.42 M, and the sample was overlayed with 0.25 M sucrose and centrifuged at 82,000 g for 60 min (step 3). The pellicle at the interface was collected, resuspended in 0.25 M sucrose, and centrifuged at 100,000 g for 10 min (step 4). The final pellet (plasma membrane fraction) was resuspended in sonication buffer (step 5). According to Hoffmann et al. (2005), the post-nuclear fraction obtained in step 2 was centrifuged at 39,000 g for 45 min to sediment mitochondria and residual plasma membrane (step 6). The supernatant, corresponding to the cytoplasmic fraction, was centrifuged at 100,000 g for 60 min (step 7) to separate the cytosolic soluble fraction from the light membrane pellet, which was further suspended in extraction medium (step 8). To clean mitochondria from plasma membrane contamination, the pellet of step 6 was resuspended in 1.38 M STM buffer, overlayed with 0.25 M sucrose, and centrifuged at 57,000 g for 90 min. The pellicle at the interface was discarded and the mitochondrial pellet was resuspended in extraction buffer (step 9). Protein concentrations of the different subcellular fractions were determined by the Lowry method using BSA as standard.

When indicated, mitochondria were treated with digitonin to strip away proteins associated with the outer membrane (Gallet et al. 1999). Briefly, mitochondria were resuspended to 30 mg/ml in 270 mM sucrose, 10 mM Tris–HCl pH 7.3, and crystallized digitonin was added to a final concentration of 0.18 mg/ml. After incubation on ice for 10 min with stirring, 10 volumes of 270 mM sucrose, 10 mM Tris–HCl pH 7.3 were added to dilute the digitonin. The mixture was then centrifuged at 12,000 g for 15 min, the pellet was washed twice in the same buffer and finally resuspended in extraction buffer.

Western blot analysis

Aliquots of total homogenate (obtained by SDS lysis), plasma membrane (step 5), cytoplasm (step 7), cytosol (step 8 supernatant), light membranes (step 8 pellet) and mitochondria (step 9) were separated by electrophoresis in

a 15% SDS–polyacrylamide gel under reducing conditions. Proteins were transferred to nitrocellulose membranes, which were incubated at room temperature for 1–2 h in 5% non-fat dry milk in PBS containing 0.1% Tween 20 (PBS–Tween). The membranes were incubated overnight at 4 °C in PBS–Tween containing 5% non-fat dry milk with mouse anti-IF_1 (1:2,000), mouse anti-OSCP (1:2,000), mouse anti-CaM (1:500), and rabbit anti-β (1:2,000). Rabbit anti-AIF (1:4,000), rabbit anti-RAIDD (1:500) and mouse anti-α_1 Na^+K^+ATPase subunit (1:2,500) were used as controls to reveal known markers of mitochondria, cytoplasm and plasma membrane (Shearwin-Whyatt et al. 2000), respectively. The membranes were washed three times in PBS–Tween and incubated in HRP-conjugated goat anti-mouse IgG (1:5,000) or anti-rabbit IgG (1:10,000). The membranes were rinsed in PBS–Tween, incubated with Pierce SuperSignal Dura chemiluminescence substrate and visualized with Image Scanner (Amersham). Signal intensities were quantified using ImageQuant TL program (GE Healthcare, Little Chalfont, Buckinghamshire, England).

To determine the subcellular distributions of IF_1 and subunits β and OSCP, signal intensities were corrected by an ad hoc procedure that took into consideration the fact that the cellular fractionation procedure maximized purity rather than yield. Specifically, we first estimated the theoretical quantity (in micrograms protein) of each subcellular fraction in the total homogenate by dividing the slope (fluorescence units per micrograms, FU/μg) of the standard curve for each marker protein in the total homogenate by that in its relevant fraction. Then, on a gel in which three quantities of each subcellular fraction and of total homogenate were immunoblotted simultaneously, we calculated the slopes for each marker protein and each experimental protein in all four cell preparations. These slopes were corrected by multiplication with the estimated theoretical quantity of the corresponding cellular fraction. The resulting values (FU) for each subcellular fraction were then expressed as percentage of that in total homogenate. The results from ten gels were expressed as mean (SD).

Results

Immunofluorescence localization of F_0F_1 subunits, IF_1 and CaM in HepG2 cells

When intact fixed HepG2 cells were incubated with a monoclonal antibody against F_0 subunit OSCP and then analyzed by flow cytometry, we observed a substantial increase in fluorescence intensity compared to cells incubated with only secondary antibody (Fig. 1a, light blue and black traces, respectively). Similar results were observed when cells were labelled with a polyclonal antibody against F_1 subunit β (Fig. 1b, dark blue and black traces, respectively). These observations confirm previous evidence for cell surface expression of F_0F_1 subunits by HepG2. Moreover, flow cytometry provided new evidence

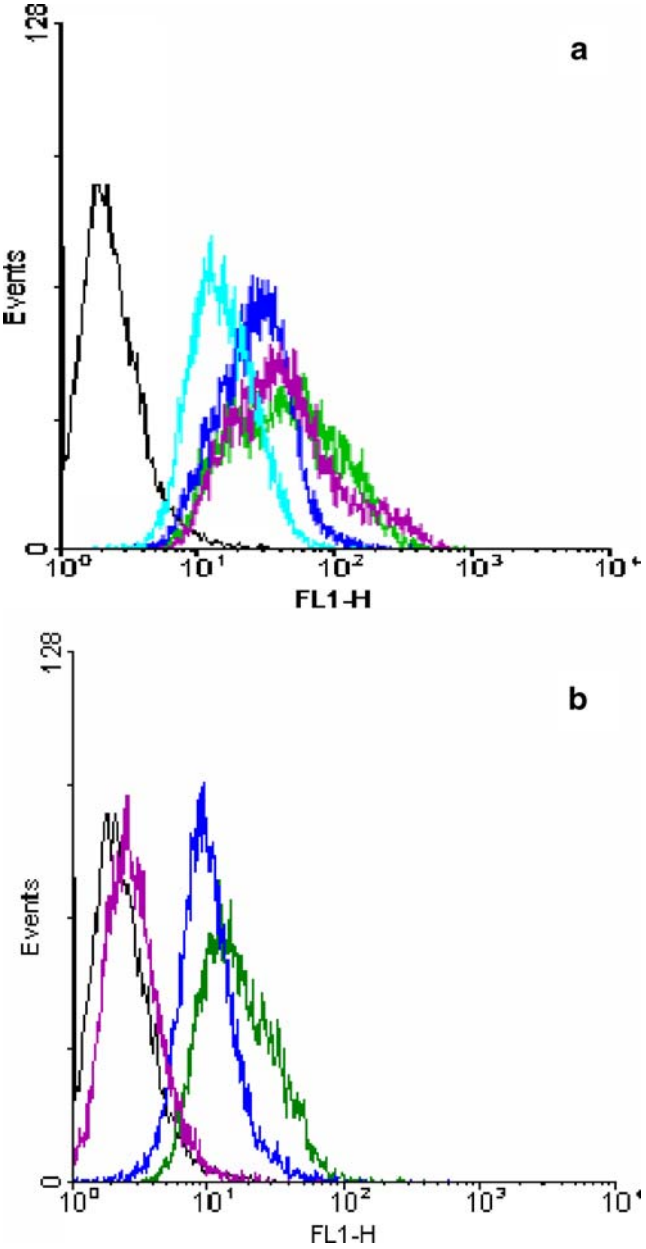

Fig. 1 Flow cytometric analysis of F_0F_1 subunits, IF_1 inhibitory protein, and Ca^{2+}–CaM on the surface of intact, fixed HepG2 cells. **a** Monoclonal antibodies. Cells were labelled with FITC-conjugated anti-mouse IgG only (negative control, *black trace*), or with anti-IF_1 (*green trace*), anti-Ca^{2+}–CaM (*dark blue trace*), anti-OSCP (*light blue trace*) or anti-α_1 subunit of Na^+K^+ATPase (*purple trace*) prior to secondary antibody treatment. **b** Polyclonal antibodies. Cells were labelled with FITC-conjugated anti-rabbit IgG only (*black trace*), or with anti-IF_1 (*green trace*), anti-β (*dark blue trace*) or anti-AIF (*purple trace*), prior to secondary antibody treatment. α_1 Subunit of Na^+K^+ATPase was positive control for plasma membrane labelling, while AIF (mitochondrial protein) was negative control

for the expression of inhibitor protein IF_1 on HepG2 plasma membrane, as revealed with both monoclonal (Fig. 1a, green trace) and polyclonal antibodies (Fig. 1b, green trace). Furthermore, as shown in Fig. 1a (dark blue trace), HepG2 cells also express Ca^{2+}–CaM on the cell surface.

Flow cytometric evidence for the cell surface expression of two F_0F_1 subunits as well as IF_1 inhibitory protein was then confirmed by the patchy and punctate staining of fixed intact HepG2 cells observed at confocal microscopy of (Fig. 2). No immunofluorescent signal was detected on cells labelled with anti-AIF antibody, confirming that mitochondria remained intact during the procedure; in addition, no signal was detected on cells labelled only with secondary antibody (data not shown). When cells were doubly labelled with anti-IF_1 and anti-OSCP or anti-β antibodies, the yellowish-orange punctate staining was indicative of colocalization of IF_1 with both F_0F_1 subunits complex. A weaker colocalization of IF_1 with α_1 subunit of Na^+K^+ATPase was observed.

To confirm that the two F_0F_1 subunits as well as IF_1 inhibitory protein are expressed in HepG2 cells at the mitochondrial level, we performed confocal microscopy on permeabilized cells that had previously been treated with Mitotracker Red mitochondrial stain (Fig. 3). Immunohistochemical detection of IF_1, β (F_1 subunit) and OSCP (F_0 subunit) revealed a strong punctate pattern matching that observed for the mitochondrial stain; yellow-orange color on merged images confirmed the localization of these proteins in mitochondria. However, when compared to the immunohistochemical pattern observed for AIF, a mitochondrial intermembrane space protein, for IF_1, β and OSCP we also observed a faint, diffuse signal suggesting that minor amounts of these proteins may be present in cytoplasm.

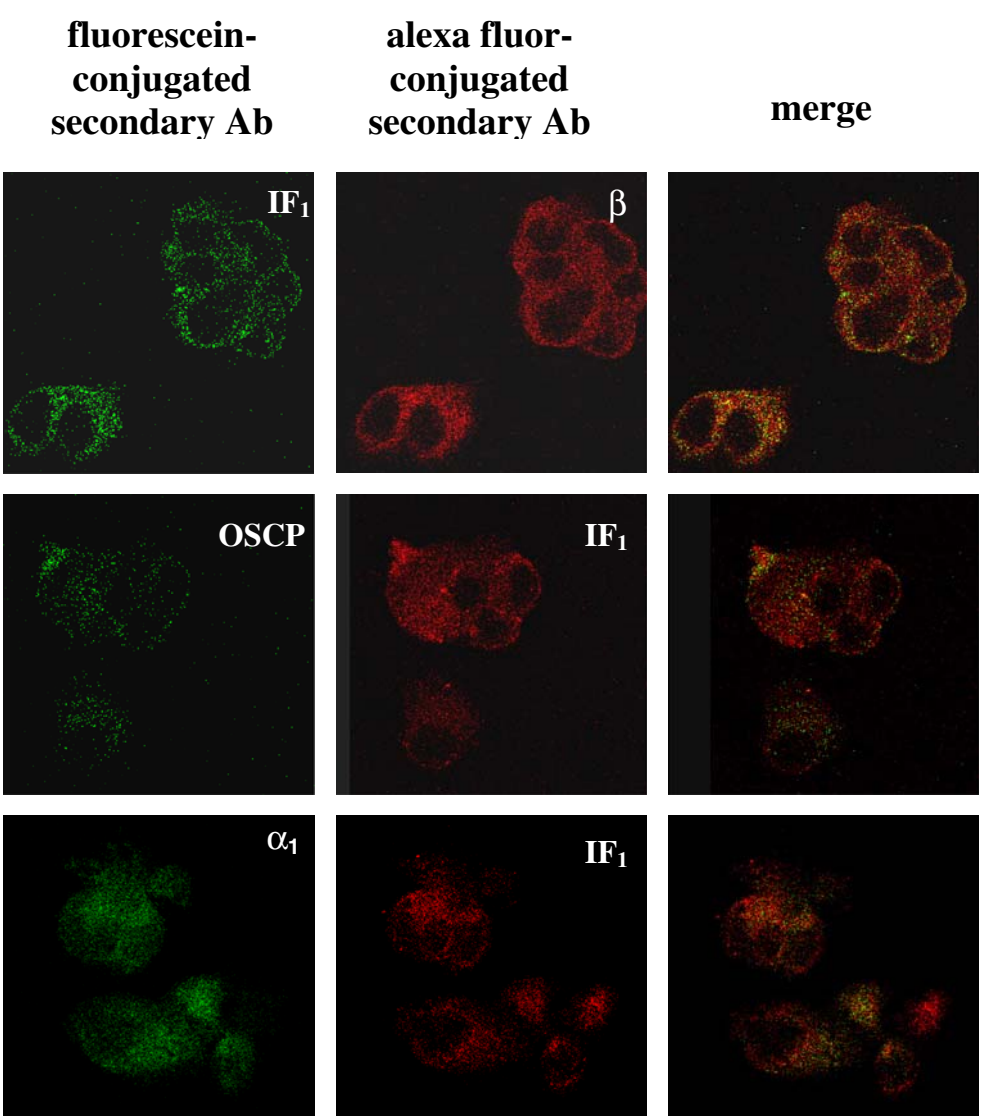

Fig. 2 Confocal microscopy of F_0F_1 subunits, IF_1 inhibitory protein, and α_1 subunit of Na^+K^+ATPase on the surface of intact, fixed HepG2 cells. Cells were doubly labelled with one monoclonal and one polyclonal antibody, and labelling was detected with FITC-conjugated goat anti-mouse IgG and alexa fluor-conjugated goat anti-rabbit IgG. α_1 Subunit of Na^+K^+ATPase was positive control for plasma membrane labelling

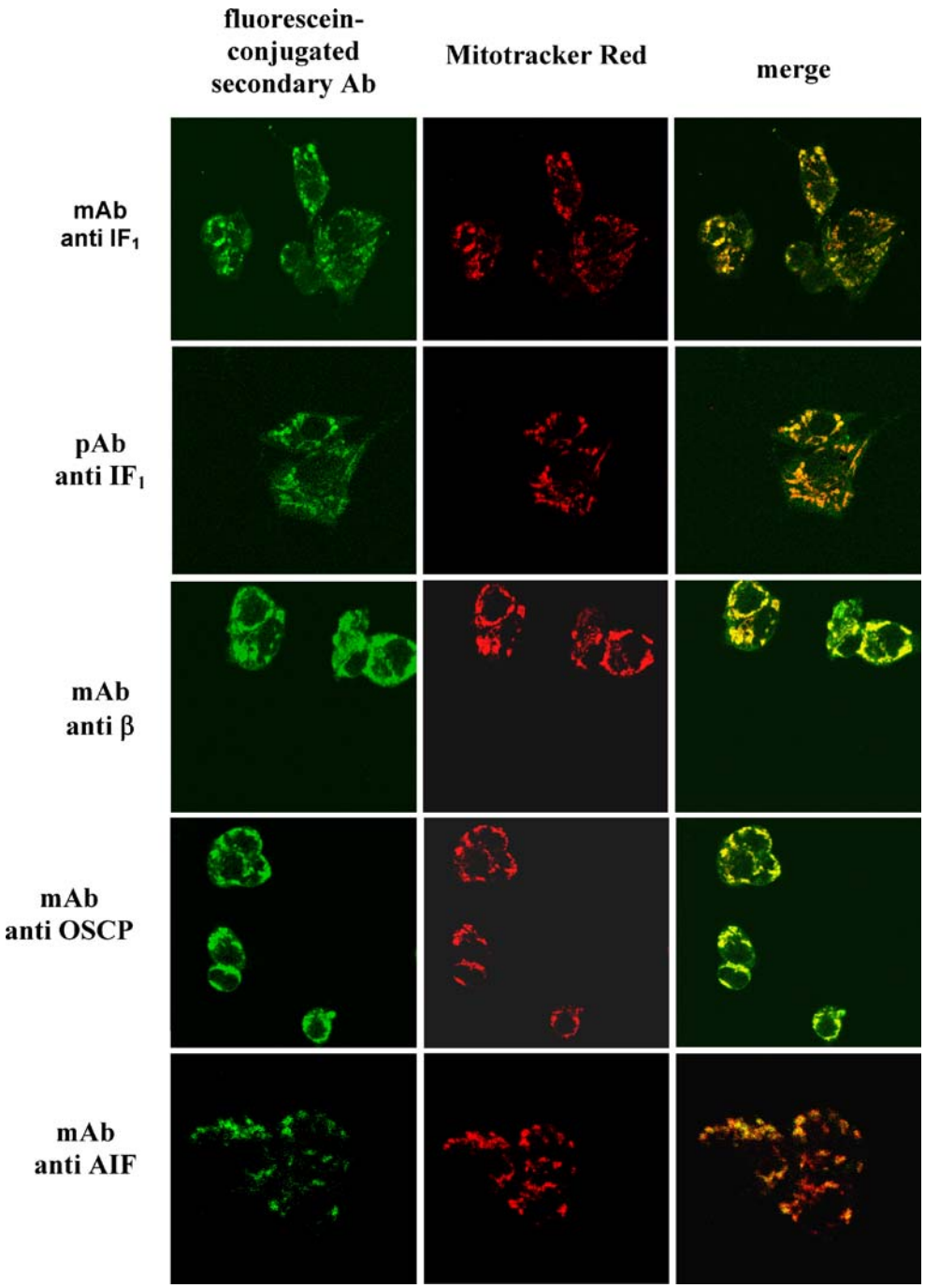

Fig. 3 Intracellular localization of IF_1 inhibitory protein and F_0F_1 subunits in HepG2 cells. HepG2 cells were labeled with mitochondrial dye Mitotracker Red, fixed and permeabilized before incubation with mono- and polyclonal anti-IF_1, anti-β or anti-OSCP, followed by detection with FITC-conjugated secondary antibodies. The yellowish-orange color in merged images indicates colocalization of the two fluorophores. Anti-AIF was used as positive control for mitochondrial staining

Colocalization of CaM and IF_1 in HepG2 cells

The presence of Ca^{2+}–CaM on the external surface of HepG2 cells, revealed by flow cytometry (Fig. 1a), was confirmed by confocal microscopy on fixed, intact cells (Fig. 4a). Moreover, dual staining provided clear evidence for colocalization of Ca^{2+}–CaM with IF_1 on the plasma membrane. In permeabilized HepG2 (Fig. 4b), diffuse staining throughout the cells indicated that Ca^{2+}–CaM is ubiquitously present in both cytoplasm and nucleus. The mostly red-and-green staining (with only hints of orange) of cells labelled with both anti-Ca^{2+}–CaM and anti-IF_1 antibodies suggests that these two proteins do not colocalize within HepG2 cells. When cells were doubly labelled with anti-Ca^{2+}–CaM antibody and Mitotracker Red, some yellow-orange signal was detected on the merged image. However, it was not clear if the two fluorescence labels both localize on the mitochondrial outer membrane or inside the organelle or if the orange color was due to the sum of the outer membrane-external CaM signal with the matrix Mitotracker Red.

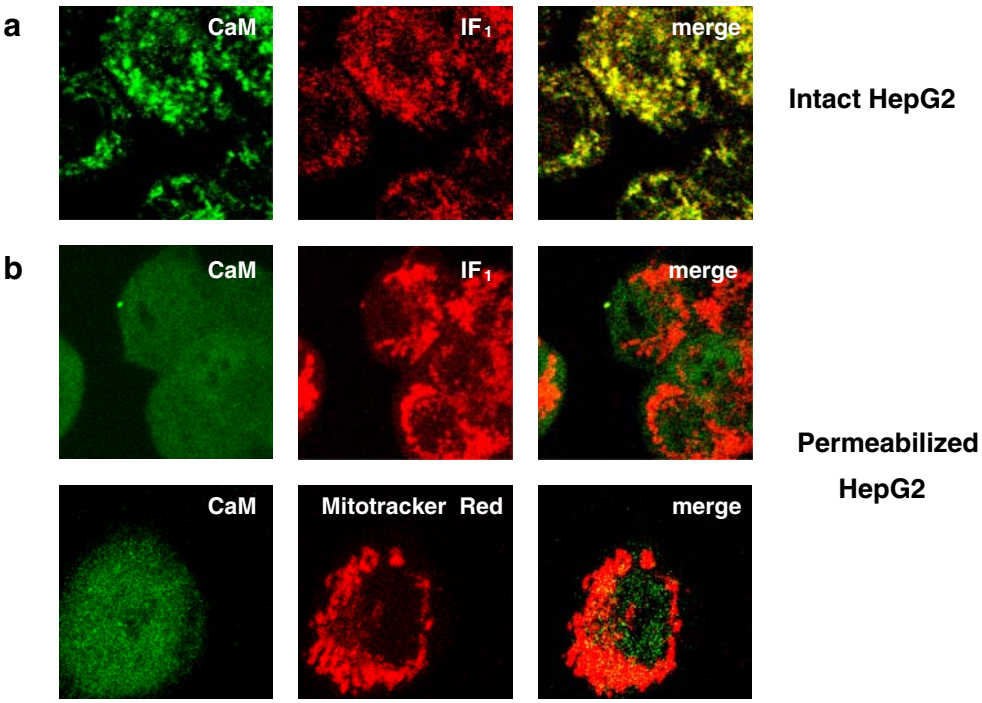

Fig. 4 Localization of CaM and IF_1 in intact and permeabilized HepG2. **a** Intact HepG2, labelled with monoclonal anti-Ca^{2+}–CaM and polyclonal anti-IF_1, followed by detection with FITC-labelled goat anti-mouse IgG and alexa fluor-conjugated goat anti-rabbit IgG. Merged image indicates colocalization of CaM and IF_1 on the cell surface. **b** HepG2, treated without or with Mitotracker Red, were fixed and permeabilized prior to immunolabelling. Merged images are inconclusive for colocalization of CaM and IF_1 at the mitochondrial level

Western blot analysis of protein distribution in HepG2 subcellular fractions

To clarify the cellular compartmentalization of the two F_0F_1 subunits as well as IF_1, we performed Western blot analysis on subcellular fractions of sonicated HepG2 cells. Purity of the mitochondrial, cytoplasmic and plasma membrane fractions was judged to be good, on the basis of low cross-contamination of marker proteins AIF, RAIDD and α_1 subunit of Na^+K^+ATPase, respectively (Fig. 5a). Differently, F_0F_1 subunits and IF_1 were found in more than one subcellular compartment (Fig. 5b). In particular, both ATPsynthase subunits were clearly detected in mitochondrial and plasma membrane fractions, but not in the cytoplasm. Instead, IF_1 was found in noticeable amounts in all three compartments. Further fractionation of cytoplasm into cytosol and light membrane (microsome) fractions (Fig. 5c) revealed that IF_1 was present in both, with an approximate ratio of 2:1 in favor of cytosol. The abundance of IF_1 in cytoplasm by Western blotting is not fully concordant with its faint immunohistochemical signal in permeabilized cells (Figs. 3 and 4b).

Semiquantitative analysis of Western blots (Table 1) confirmed the purity of the mitochondrial, cytoplasmic and plasma membrane fractions. There was some cross-contamination (<10%) of plasma membrane in the cytoplasmic fraction, and mitochondria in the plasma membrane fraction, but over 99% of cytoplasmic marker RAIDD was recovered in the corresponding fraction. Regarding F_0F_1 subunits, semiquantitative analysis confirmed that both OSCP and β were distributed between mitochondria and plasma membrane, with cytoplasmic values at the level of detection. Moreover, this analysis indicated that approximately half of immunochemically detected IF_1 was localized to mitochondria and the rest was divided between cytoplasm and plasma membrane. Considering that immunohistochemical analysis of permeabilized HepG2 cells gave evidence only for low levels of cytoplasmatic IF_1, the finding of 23.79% of total IF_1 in this subcellular compartment should be interpreted with caution.

Western blotting was also used to clarify earlier immunohistochemical results on the colocalization of CaM with the mitochondrial marker Mitotracker Red. As shown in Fig. 6a, CaM was detected in cytoplasmic and plasma membrane fractions, confirming earlier results with flow cytometry and confocal microscopy. Moreover, a strong CaM signal was detected in whole mitochondria, but no signal was found in digitonin-treated mitochondria. These results indicate that CaM is weakly associated with the external surface of the outer mitochondrial membrane and is not present at detectable levels in the mitochondrial matrix or intermembrane space. Similar experiments performed with AIF, β and IF_1 antibodies demonstrated that the integrity of the mitochondrial outer and inner membranes had been preserved (Fig. 6b).

Discussion

With this research, we found a relevant amount of IF_1 on the plasma membrane of HepG2 cells, where we also documented the presence of Ca^{2+}–CaM and OSCP and β

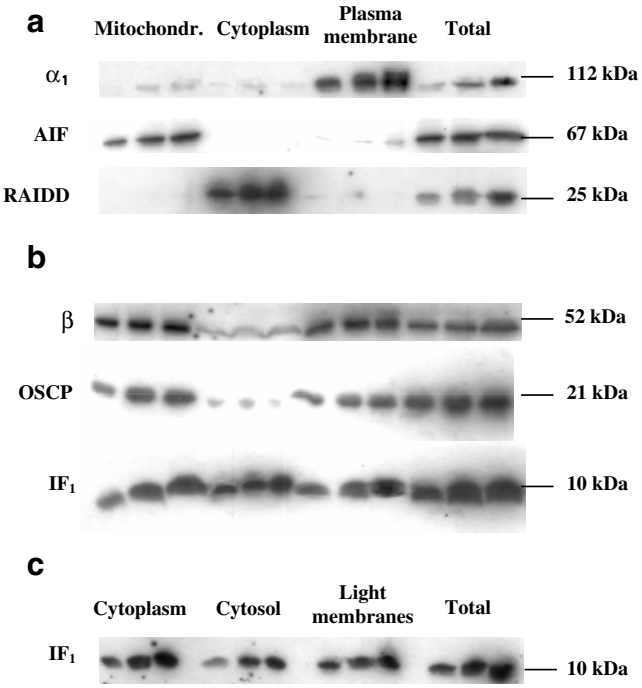

Fig. 5 Western blot of F_0F_1 subunits and IF_1 in HepG2 subcellular fractions. **a** Subcellular fraction marker proteins: AIF (mitochondria), α_1 subunit of Na^+K^+ATPase (plasma membrane) and RAIDD (cytoplasm). *From left to right* Mitochondrial fraction, 20, 40 and 60 μg protein; cytoplasmic fraction, 100, 125 and 150 μg; plasma membrane fraction, 15, 30, 45 μg; and total homogenate, 30, 60, 90 μg. **b** F_0F_1 subunits β and OSCP, and IF_1. Samples are the same as in **a**. **c** Immunochemical detection of IF_1 in cytoplasmic subfractions. *From left to right* Total cytoplasmic fraction, 30, 60, 90 μg; cytosolic soluble fraction, 50, 80, 110 μg; light membranes (microsomes), 40, 70, 100 μg; and total homogenate, 10, 20, 30 μg

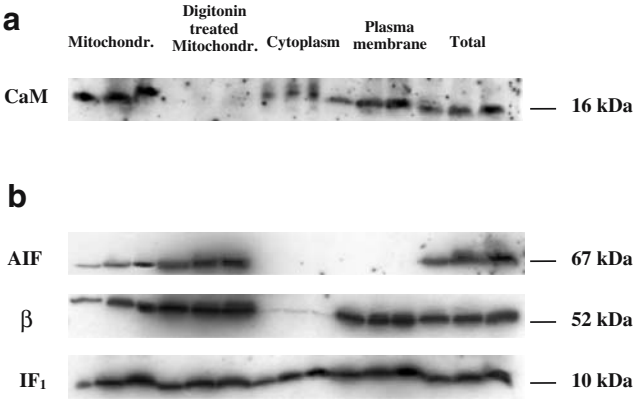

Fig. 6 Western blot of CaM in HepG2 subcellular fractions. **a** CaM is present in mitochondrial, cytoplasmic and plasma membrane fractions of HepG2 cells, but is absent from mitochondria which have been stripped of outer membrane proteins by digitonin. **b** Digitonin treatment did not result in loss of three proteins located in the intermembrane space (AIF) or matrix (β and IF_1) confirming that mitochondrial integrity was preserved. *From left to right* Mitochondrial fraction, 20, 40, 60 μg protein; digitonin-treated mitochondria, 20, 40, 60 μg; cytoplasmic fraction, 90, 120, 150 μg; plasma membrane fraction, 15, 30, 45 μg; and total homogenate, 30, 60, 90 μg

subunits of ecto–F_0F_1ATPsynthase. Moreover, we observed that, on plasma membrane but not in mitochondria, IF_1 colocalizes with Ca^{2+}–CaM.

This study provides the first evidence of endogenous IF_1 on the cell surface of HepG2 cells. Thus far, ecto–IF_1 has been identified only on endothelial cells (Burwick et al. 2005; Cortes-Hernandez et al. 2005). Moreover, by documenting the presence of β and OSCP subunits of F_0F_1ATPsynthase on the cell surface, we confirmed previous findings that ecto–F_0F_1ATPsynthase is expressed by rat hepatocytes (Martinez et al. 2003) and HepG2 cells (Bae et al. 2004). Like Bae et al. (2004), we found that the immunohistochemical staining for β and OSCP subunit was patchy and punctate, typical of plasma membrane lipid raft proteins; we obtained similar staining patterns for CaM and IF_1, suggesting that also these proteins associate in lipid rafts. Our finding that HepG2 cells express CaM on the plasma membrane, documented with both immunofluorescence and Western blotting techniques, agrees with earlier reports of CaM in the plasma membrane fraction of rat liver (Harper et al. 1980) and on the cell surface of rat heart muscle (Nakagawa et al. 1990). To our knowledge, since these earlier reports, plasma membrane CaM has not been further discussed or characterized. Such localization is, however, not surprising considering that CaM plays a key role in regulating general membrane trafficking (Horwitz et al. 1981; Grasso et al. 1990; DiPaola et al. 1984; Apodaca et al. 1994; Hunziker 1994; Colombo et al. 1997; Rizzo et al. 1998).

In hepatic cells, ecto–F_0F_1ATPsynthase has been shown to function as apoA–I receptor and to trigger HDL_2 endocytosis concomitant with the extracellular hydrolysis of ATP (Martinez et al. 2003). Addition of exogenous IF_1 to these cells markedly reduced endocytosis as well as ATP hydrolysis by ecto–F_0F_1ATPsynthase under both basal and apoA–I-stimulated conditions (Martinez et al. 2003). Thus,

Table 1 Percentage distributions of subcellular fraction markers, ATPsynthase subunits β and OSCP, and inhibitory protein IF_1

Protein	Mitochondria	Cytoplasm	Plasma membrane
α_1	2.39 (2.47)	9.11 (6.50)	88.2 (4.40)
AIF	86.2 (3.10)	4.26 (2.21)	9.24 (4.03)
RAIDD	0.28 (0.31)	99.06 (0.40)	0.34 (0.54)
β	54.25 (5.72)	4.67 (5.21)	33.77 (5.36)
OSCP	53.51 (5.24)	4.53 (1.97)	38.61 (6.73)
IF_1	49.39 (6.60)	23.79 (4.66)	17.63 (5.72)

Values are means (SD) of 12–40 densitometric determinations (ten gels), and are expressed as the percentage of the signal observed in each subcellular compartment with respect to that in the total homogenate after correction for the yield of each compartment after subcellular fractionation.

α_1 Subunit of Na^+K^+ATPase (plasma membrane marker), *AIF* apoptosis-inducing factor (mitochondrial marker), *RAIDD* RIP-associated ICH-1 homologous protein with a death domain (cytoplasmic marker)

in vivo, translocation of endogenous IF_1 to the cell surface and binding to the ecto–F_0F_1 complex may be a cellular mechanism for regulating endocytosis. The fact that exogenous IF_1 modulated ecto–F_0F_1ATPsynthase activity in these cells suggests that the plasma membrane enzyme is not saturated with its inhibitor protein. This may be explained, at least in part, by competition between CaM and ecto–F_0F_1ATPsynthse for IF_1 binding (Contessi et al. 2005). In accordance, differently from IF_1–F_1 binding (Contessi et al. 2004), CaM complex with IF_1 forms also at neutral pH characteristic of the extracellular space in normal tissues.

In support of this hypothesis, immunofluorescence experiments provided strong evidence that, on HepG2 plasma membrane, IF_1 colocalizes with CaM. The IF_1–Ca^{2+}–CaM complex has been previously described by Pedersen and Hullihen (1984) and by Schwerzmann et al. (1985) and was further characterized by us (Contessi et al. 2005). The present study provides the first evidence, though indirect, that this complex can form on the external surface of cells, where Ca^{2+} concentration is in the millimolar range, and suggests that CaM functions as sequester of ecto–IF_1, thereby modulating the availability of IF_1 to bind to and regulate ecto–F_0F_1ATPsynthase. This hypothesis is supported by the facts that binding of IF_1 to either CaM or soluble F_1-ATPase is mutually exclusive and that a target sequence is located inside the minimal inhibitory sequence of IF_1 (Contessi et al. 2005).

In contrast to the clear colocalization of CaM and IF_1 on HepG2 plasma membrane, we did not obtain evidence for an interaction between the two proteins within the cell. Although CaM was found to be abundant in HepG2 cytoplasm, the presence of IF_1 in the cytoplasm was not unequivocally demonstrated. Western blot analysis indicated that 23.79% of total cellular IF_1 is located in the cytoplasm, but immunohistochemical analysis revealed only a faint cytoplasmic signal for IF_1. Since it is possible that the strong cytoplasmic CaM signal obscured a faint, diffuse IF_1 signal, we can not exclude the possibility that the two proteins can also interact in the cytoplasm. However, we must also consider that the Western blot detection of IF_1 in the cytoplasm may have been due to an experiment artefact, in which IF_1 may have dissociate from the plasma membrane during subcellular fractionation. If this is the case, then this results would imply that half of all cellular IF_1 is associated with the plasma membrane.

Our study also did not provide clear evidence for an interaction between CaM and IF_1 at the mitochondrial level. Merged microscopic images of permeabilized HepG2 cells labelled with both anti-Ca^{2+}–CaM and anti-IF_1 antibodies gave a reddish-orange color, not fully supporting a physical closeness of the two fluorophores. This color was similar to that seen on merged images of cells stained with anti-Ca^{2+}–CaM antibodies and Mitotracker Red. The association of CaM with mitochondria was clarified by Western blotting experiments which showed that CaM is present in the mitochondrial fraction of HepG2 cells but is stripped from mitochondria by digitonin treatment. Instead, digitonin treatment did not noticeably reduce the mitochondrial content of IF_1. These results indicate that CaM is associated only with the external face of the outer mitochondrial membrane, as previously suggested by Pardue et al. (1981). The absence of CaM from the mitochondrial matrix and intermembrane space, as reported here, is the subject of debate: earlier reports suggested its localization inside mitochondria (Hatase et al. 1982; Schnaitman and Greenawalt 1968) while more recent data tend to exclude it (Moriya et al. 1993; Nakazawa 2001; Milikan and Bolsover 2000; Lopez et al. 2000).

Together, these experiments provide evidence that IF_1 and CaM can interact on the plasma membrane of HepG2 cells but not inside mitochondria. Moreover, our results suggest that plasma membrane Ca^{2+}–CaM competes with ecto–ATPsynthase for IF_1 binding, thus providing a mechanism for regulating the hydrolytic activity of ecto–ATPsynthase.

In conclusion, the data reported here provide evidence that, under basal conditions, IF_1 is present on the external surface of HepG2 cells. This observation is the basis for hypothesizing the existence of a regulatory mechanism, in which IF_1 is sequestered by CaM on the plasma membrane. The latter mechanism, supported by evidence of IF_1 colocalization with CaM on the surface of HepG2 cells, could serve to generate extracellular ADP and sustain the endocytotic process in which ecto–ATPsynthase is involved (Martinez et al. 2003). Our experiments shed some light on the physiological role of IF_1–Ca^{2+}–CaM, but further in vivo analyses are required to discover and define the functions of this protein complex.

Acknowledgement We thank Dr. D. A. Harris (Department of Biochemistry, University of Oxford, UK), Dr. F. Dabbeni-Sala (Department of Pharmacology, University of Padua, Italy), and Prof. C. Brancolini (Department of Biomedical Sciences and Technologies, University of Udine, Italy) for kindly providing polyclonal anti-IF_1, anti-β subunit and anti-RAIDD antibodies, respectively. This work was supported by MIUR, PRIN 2004. Scientific editing of the manuscript was provided by Valerie Matarese.

References

Abou-Khalil S, Abou-Khalil WH, Planas L, Tapiero H, Lampidis TJ (1985) Biochem Biophys Res Commun 127:1039–1044

Apodaca G, Enrich C, Mostov KE (1994) J Biol Chem 269:19005–19013

Bae TJ, Kim MS, Kim JW, Kim BW, Choo HJ, Lee JW, Kim KB, Lee CS, Kim JH, Chang SY, Kang CY, Lee SW, Ko YG (2004) Proteomics 4:3536–3548

Boyer PD (1997) Annu Rev Biochem 66:717–749

Burwick NR, Wahl ML, Fang J, Zhong Z, Moser TL, Li B, Capaldi RA, Kenan DJ, Pizzo SV (2005) J Biol Chem 280:1740–1745
Cabezon E, Montgomery MG, Leslie AG, Walker JE (2003) Nat Struct Biol 10:744–750
Champagne E, Martinez LO, Collet X, Barbaras R (2006) Curr Opin Lipidol 17:279–284
Chin D, Means AR (2000) Trends Cell Biol 10:322–328
Colombo MI, Beron W, Stahl PD (1997) J Biol Chem 272:7707–7712
Comelli M, Metelli G, Mavelli I (2007) Am J Physiol (Heart Circ Physiol) 292(2):H820–829
Contessi S, Metelli G, Mavelli I, Lippe G (2004) Biochem Pharmacol 67:1843–1851
Contessi S, Haraux F, Mavelli I, Lippe G (2005) J Bioenerg Biomembranes 37:317–326
Cortes-Hernandez P, Dominguez-Ramirez L, Estrada-Bernal A, Montes-Sanchez DG, Zentella-Dehesa A, de Gomez-Puyou MT, Gomez-Puyou A, Garcia JJ (2005) Biochem Biophys Res Commun 330:844–849
Di Pancrazio F, Mavelli I, Isola M, Losano G, Pagliaro P, Harris DA, Lippe G (2004) Biochim Biophys Acta 1659:52–62
DiPaola M, Keith CH, Feldman D, Tycko B, Maxfield FR (1984) J Cell Physiol 118:193–202
Gallet PF, Zachowski A, Julien R, Fellmann P, Devaux PF, Maftah A (1999) Biochim Biophys Acta 1418:61–70
Grasso JA, Bruno M, Yates AA, Wei L, Epstein PM (1990) Biochem J 266:261–272
Green DW, Grover GJ (2000) Biochim Biophys Acta 1458:343–355
Harper JF, Cheung WY, Wallace RW, Huang HL, Levine SN, Steiner AL (1980) Proc Natl Acad Sci 77:366–370
Hatase O, Tokuda M, Itano T, Matsui H, Doi A (1982) Biochem Biophys Res Commun 104:673–679
Hoffmann K, Blaudszun J, Brunken C, Hopker WW, Tauber R, Steinhart H (2005) Anal Bioanal Chem 381:1138–1144
Horwitz SB, Chia GH, Harracksingh C, Orlow S, Pifko-Hirst, Schneck J, Sorbara L, Speaker M, Wilk EW, Rosen OM (1981) J Cell Biol 91:798–802
Hunziker W (1994) J Biol Chem 269:29003–29009
Jacquet S, Malaval C, Martinez LO, Sak K, Rolland C, Perez C, Nauze M, Champagne E, Terce F, Gachet C, Perret B, Collet X, Boeynaems JM, Barbaras R (2005) Cell Mol Life Sci 62: 2508–2515
Joza N, Susin SA, Daugas E, Stanford WL, Cho SK, Li CY, Sasaki T, Elia AJ, Cheng HY, Ravagnan L, Ferri KF, Zamzami N, Wakeham A, Hakem R, Yoshida H, Kong YY, Mak TW, Zuniga-Pflucker JC, Kroemer G, Penninger JM (2001) Nature 410:549–554
Lopez MF, Kristal BS, Chernokalskaya E, Lazarev A, Shestopalov AI, Bogdanova A, Robinson M (2000) Electrophoresis 21:3427–3440
Martinez LO, Jacquet S, Esteve JP, Rolland C, Cabezon E, Champagne E, Pineau T, Georgeaud V, Walker JE, Terce F, Collet X, Perret B, Barbaras R (2003) Nature 421:75–79
Milikan JM, Bolsover SR (2000) Pflugers Arch 439:394–400
Moriya M, Katagiri C, Yagi K (1993) Cell Tissue Res 271:441–451
Moser TL, Stack MS, Asplin I, Enghild JJ, Hojrup P, Everitt L, Hubchak S, Schnaper HW, Pizzo SV (1999) Proc Natl Acad Sci 96:2811–2816
Moser TL, Kenan DJ, Ashley TA, Roy JA, Goodman MD, Misra UK, Cheek DJ, Pizzo SV (2001) Proc Natl Acad Sci 98:6656–6661
Nakagawa R, Qiao Y, Asano G (1990) Nippon Ika Daigaku Zasshi 57:541–546
Nakazawa K (2001) Heart Res 151:133–140
Pardue RL, Kaetzel MA, Hahn SH, Brinkley BR, Dedman JR (1981) Cell 23:533–542
Pedersen PL, Hullihen J (1984) J Biol Chem 259:15148–15153
Penna C, Pagliaro P, Rastaldo R, Di Pancrazio F, Lippe G, Gattullo D, Mancardi D, Samaja M, Losano G, Mavelli I (2004) Am J Physiol Heart Circ Physiol 287:H2192–2200
Rizzo V, McIntosh DP, Oh P, Schnitzer JE (1998) J Biol Chem 273:34724–34729
Schnaitman C, Greenawalt JW (1968) J Cell Biol 38:158–175
Schwerzmann K, Muller M, Carafoli E (1985) Biochim Biophys Acta 816:63–67
Scotet E, Martinez LO, Grant E, Barbaras R, Jeno P, Guiraud M, Monsarrat B, Saulquin X, Maillet S, Esteve JP, Lopez F, Perret B, Collet X, Bonneville M, Champagne E (2005) Immunity 22:71–80
Shearwin-Whyatt LM, Harvey NL, Kumar S (2000) Cell Death Differ 7:155–165
Tietz P, Jefferson J, Pagano R, Larusso NF (2005) J Lipid Res 46:1426–1432
Walker JE, Gay NJ, Powell SJ, Kostina M, Dyer MR (1987) Biochemistry 26:8613–8619
Yamniuk AP, Vogel HJ (2004) Mol Biotechnol 27:33–57 (Review)
Zhao H, Hundal HS (2000) Biochem Biophys Res Commun 274:43–48